# Phosphorus Analogues of Diazonium Ions. Stabilities, Spectroscopic Properties, and Electronic Structures of the P Analogues of Methyldiazonium Ion
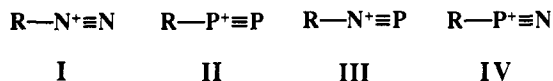
**Rainer Glaser,*** **Christopher J. Horan, Godwin Sik-Cheung Choy, and Benjamin L. Harris**

*Department of Chemistry, University of Missouri, Columbia, Missouri 65211 (Received: October 4, 1991; In Final Form: December 23, 1991)*

The P analogues of methyldiazonium ion $(CH_3NN)^+$ (**1**), methyldiphosphonium ion $(CH_3PP)^+$ (**2**), methylphosphoazonium ion $(CH_3NP)^+$ (**3**), and methylazophosphonium ion $(CH_3PN)^+$ (**4**) were studied with ab initio techniques. Potential energy surface analysis shows that the $C_{3v}$-symmetric ions all are minima. **4** corresponds to a shallow minimum along the automerization path of its isomer **3**. A bridged structure of **2** exists as a local minimum along the automerization path, and this automerization occurs within a tightly bonded ion–molecule complex with small activation barriers. Methyl cation affinities of 43.0, 71.3, 100.4, and 42.1 kcal/mol were determined for the formations of **1**–**4**, respectively, at MP4(fc,sdtq)/6-311G(df,p)//MP2-(full)/6-311G(df,p) and including MP2(full)/6-31G(d) vibrational zero-point energies. The thermodynamic stabilities of **2** and **3** with regard to the dissociations $(CH_3XY)^+ \rightarrow CH_3^+ + XY$ might be affected by exothermic XY oligomerization and the reactions $(CH_3PP)^+ \rightarrow CH_3^+ + \frac{1}{2}P_4$ and $(CH_3NP)^+ \rightarrow CH_3^+ + \frac{1}{3}D_{3h}$ $(PN)_3$ were studied. Ions **2** and **3** are predicted to be more stable toward dissociation than **1**. These results suggest that **2** and **3** should be detectable in the gas phase and possibly also in superacidic media. Like its aryl analogue, **3** might be accessible synthetically. Spectroscopic properties including IR spectra, dipole and quadrupole moments, rotational constants, and polarizabilities are reported that may assist in their detection. Electronic structures of **1**–**4** were studied in a variety of ways. A new energy decomposition method related to the definition of the electron density difference function, $\Delta\rho = \rho(CH_3XY^+) - \rho^M(CH_3^+) - \rho^M(XY)$, is presented. Charge distributions in **1**–**4** are discussed with regard to the Lewis notations. CN- and CP-bonded ions clearly show distinct bonding patterns.

## Introduction

Replacement of N by P in **I** may lead to **II**–**IV**. The ions **II** might be called diphosphonium ions in analogy to **I**. Considering the formal charges in the Lewis structures shown, **III** and **IV** might be called phosphoazonium and azophosphonium ions, respectively. Aromatic diazonium ions are well-known and several alkyldiazonium ions[2,3] also have been characterized. Diphosphonium ions are unknown, and of the PN compounds, only two aromatic ions **III** were reported.[4]

$$R\!-\!\!N^+\!\!\equiv\!\!N \qquad R\!-\!\!P^+\!\!\equiv\!\!P \qquad R\!-\!\!N^+\!\!\equiv\!\!P \qquad R\!-\!\!P^+\!\!\equiv\!\!N$$

$$\text{I} \qquad\qquad \text{II} \qquad\qquad \text{III} \qquad\qquad \text{IV}$$

Niecke et al. recently reported the synthesis and the crystal structures of the first two representatives of **III**, namely, of [(*tert*-butyl)$_2$PSe$_2$]·(PNAr)[5] and AlCl$_4^-$·(PNAr)[6] (Ar = 2,4,6-tri-*tert*-butylphenyl). We had recently suggested[7] that the ions **II** also might be synthetically accessible, based on our studies of diazonium ions.[8–11] Electron density analysis[12] has shown that

the ions **I** are best described as carbenium ions closely associated with a strongly polarized N$_2$, and a bonding model has been proposed. Electrostatic interactions between the charge of the hydrocarbon fragment and the induced dipole moment of N$_2$ are more important for CN bonding than is the charge transfer between N$_2$ and the carbenium ion. If this bonding model were to carry over to **II**, then one might expect that the ions **II** with their more polarizable P$_2$ group might be stable. Unlike nitrogen, elemental P consists of $T_d$ P$_4$ in the solid (white P), liquid, and gas phases.[13] Moderately distorted P$_4$ units have also been found as ligands in complexes.[14,15] Measurable dissociation of P$_4$ into P$_2$ occurs in vapor above 800 °C, but only recently has it been possible to stabilize P$_2$ by complexation to transition metals.[16]

Earlier theoretical research on **I**–**IV** focused on the protonated species.[17] (HNN)$^+$ greatly prefers the linear over the symmetrically bridged structure,[18] and this ion has been identified as an intermediate in the NH$_3$ diazotization by Olah et al.[19] In contrast, Niecke et al.[20] and Nguyen and Fitzpatrick[21] found that (HPP)$^+$

(1) Presented at the Midwest Regional ACS Meeting in Omaha, NE, Nov 1991. Preliminary results presented at the 195th ACS National Meeting Toronto, Canada, June 1988.

(2) Reviews: (a) Kirmse, W. *Angew. Chem., Int. Ed. Engl.* **1976**, *415*, 251. (b) Laali, K.; Olah, G. A. *Rev. Chem. Intermed.* **1985**, *6*, 237.

(3) Alkyldiazonium ions have been observed in superacid media, and methyldiazonium ion has been studied in the gas phase. In the solid state, alkyldiazonium ions can be stabilized in transition element complexes, but the alkyldiazonium ligands greatly differ from the free ions. See ref 7 for references.

(4) *Multiple Bonds and Low Coordination in Phosphorus Chemistry*; Regitz, M., Scherer, O., Eds.; Thieme Verlag: New York, 1990.

(5) Niecke, E.; Nieger, M.; Reichert, F.; Schoeller, W. W. *Angew. Chem., Int. Ed., Engl.* **1988**, *27*, 1713.

(6) Niecke, E.; Nieger, M.; Reichert, F. *Angew. Chem., Int. Ed. Engl.* **1988**, *27*, 1715.

(7) Glaser, R. *J. Phys. Chem.* **1989**, *93*, 7993.

(8) Glaser, R. *J. Am. Chem. Soc.* **1987**, *109*, 4237.

(9) Glaser, R.; Choy, G. S.-C.; Hall, M. K. *J. Am. Chem. Soc.* **1991**, *113*, 1109.

(10) Glaser, R.; Horan, C.; Nelson, E.; Hall, M. K. *J. Org. Chem.* **1992**, *57*, 215.

(11) Glaser, R. *J. Comp. Chem.* **1990**, *11*, 663.

(12) Reviews: (a) Bader, R. F. W.; Nguyen-Dang, T. T.; Tal. Y. *Rep. Prog. Phys.* **1981**, *44*, 893. (b) Bader, R. F. W. *Acc. Chem. Res.* **1985**, *18*, 9. (c) Bader, R. F. W. *Chem. Rev.* **1991**, *91*, 893. (d) Bader, R. F. *Atoms in Molecules—A Quantum Theory*; Clarendon Press: Oxford University Press, Oxford, OX2 6DP, UK, 1990.

(13) Cotton, F. A.; Wilkinson, G. *Advanced Inorganic Chemistry*, 4th ed.; Wiley and Sons: New York, 1980; p 442.

(14) Reviews: (a) Scherer, O. P. *Angew. Chem., Int. Ed. Eng.* **1985**, *24*, 924. (b) Herrmann, W. A. *Angew. Chem., Int. Ed. Eng.* **1986**, *25*, 56. (c) Vaira, M. D.; Stoppioni, P.; Peruzzini, M. *Polyhedron* **1987**, *6*, 351.

(15) (a) [(np$^3$)Ni($\eta^1$-P$_4$)]: Dapporto, P.; Midollini, S.; Sacconi, L. *Angew. Chem., Int. Ed. Eng.* **1979**, *1*, 469. (b) [RhCl($\eta^2$-P$_4$)(PPh$_3$)$_2$]: Ginsberg, A. P.; Lindsell, W. E.; McCullough, K. J.; Sprinkle, C. R.; Welch, A. J. *J. Am. Chem. Soc.* **1986**, *108*, 403, and references therein. (c) [(Cp*)$_2$Zr($\eta^2$-P$_4$)]: Scherer, O. J. *Nachr. Chem., Tech. Lab.* **1987**, *35*, 1141.

(16) (a) Co$_2$(CO)$_5$[PPh$_3$](P$_2$): Campana, C. F.; Vizi-Orosz, A.; Palyi, G.; Marko, L.; Dahl, L. F. *Inorg. Chem.* **1979**, *18*, 3054. (b) [($\eta^5$-Cp)Mo-(CO)$_2$]$_2$P$_2$: Scherer, O. J.; Sitzmann, H.; Wolmershäuser, G. *J. Organomet. Chem.* **1984**, *268*, C9. (c) (Cp*Mo)(P$_2$)$_2$(MoCp*): Scherer, O. J.; Sitzmann, H.; Wolmershäuser, G. *Angew. Chem.* **1985**, *97*, 358; *Angew. Chem., Int. Ed. Engl.* **1985**, *24*, 351. (d) [(R$_2$P-PR$_2$)Ni]$_2$(P$_2$): Schäfer, H.; Binder, D.; Fenske, D. *Angew. Chem.* **1985**, *97*, 523; *Angew. Chem., Int. Ed. Engl.* **1985**, *24*, 522.

(17) For studies of protonated OXY, including the hydroxy derivatives, see: (a) Davy, R. D.; Schaefer, H. F., III *J. Chem. Phys.* **1990**, *92*, 5417. (b) Davy, R. D.; Xie, Y.; Schaefer, H. F., III *J. Am. Chem. Soc.* **1991**, *113*, 3697.

(18) (a) Botschwinda, P. *Chem. Phys. Lett.* **1984**, *107*, 535, and references therein. (b) Linear structure is preferred by 48.7 kcal/mol over the bridged transition-state structure at CISD/6-31G* and including VZPEs determined at that level.

(19) Olah, G. A.; Herges, R.; Felberg, J. D.; Rrakash, G. K. S. *J. Am. Chem. Soc.* **1985**, *107*, 5282.

(20) Busch, T.; Schoeller, W. W.; Niecke, E.; Nieger, M.; Westermann, H. *Inorg. Chem.* **1989**, *28*, 4334.

prefers the bridged structure by 5–8 kcal/mol.[22] Maclagan[23] recently reported proton affinities of P compounds including PN. (HNP)$^+$ was found to be more stable than (HPN)$^+$, in agreement with the earlier study by Buenker et al.,[23c] and the latter is a transition-state structure.[23b]

In this article, we report the results of a comparative theoretical study of the smallest alkyl derivatives of I–IV, the methyl systems **1–4**. The potential energy surfaces of **2–4** were explored at the MP3/6-31G*//RHF/6-31G* level, and the $C_{3v}$ structures of **1–4** and the diatomic molecules XY were studied with structural optimization at correlated levels and with well-polarized basis sets. The methylation reactions were studied and methyl cation affinities are reported.

$$CH_3^+ + XY \rightarrow (CH_3XY)^+ \qquad (X, Y = N, P)$$

The thermodynamic stabilities of **2–4** with regard to demethylation may be reduced by the exothermic oligomerizations of $P_2$ and PN, and the reactions

$$(CH_3XY)^+ \rightarrow CH_3^+ + \tfrac{1}{2}P_4$$

$$(CH_3XY)^+ \rightarrow CH_3^+ + \tfrac{1}{3}(PN)_3$$
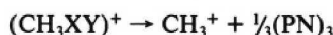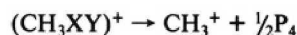
were thus also considered. The ions **2** and **3** are predicted to be stable molecules that should be detectable in the gas phase. Spectroscopic properties are reported to help in their detection. The effects of P substitution on the electronic structures of **1–4** are analyzed in a variety of ways, and an energy decomposition method related to the definition of the electron density difference function, $\Delta\rho = \rho(CH_3XY^+) - \rho^M(CH_3^+) - \rho^M(XY)$, is presented. The emerging best single representations for the charge distributions in **1–4** are discussed with regard to the valence bond representations, and the different degree is emphasized by which the "X lone pair" engages in C–X bonding.

## Computational Methods

Ab initio calculations were carried out with Gaussian88.[24] Geometries were optimized[25] within the symmetry point groups specified. Harmonic vibrational frequencies were calculated analytically to characterize stationary structures as minima or saddle points and to obtain vibrational frequencies and zero-point energies. The vibrational zero-point energy corrections calculated at the RHF level were scaled in the usual fashion[26] (factor 0.9), and those determined at the MP2 level were not scaled. Optimization and characterization of stationary structures were carried out at the RHF level with the 6-31G* basis set[27] and at the MP2(full) level[28] with the basis sets 6-31G*, 6-311G**, and 6-311G(df,p).[29] Energies were also determined with Møller–

(21) Nguyen, M. T.; Fitzpatrick, N. J. *Chem. Phys. Lett.* **1988**, *146*, 524.

(22) The bridged structure is preferred over the linear structure by 6.03 kcal/mol at the CISD/6-31G* level and including VZPEs determined at this level. The linear structure is a transition-state structure for the narcissistic isomerization of an asymmetrically bridged shallow local minimum with angle H–P–P = 147°; to be published.

(23) (a) Maclagan, R. G. A. R. *J. Phys. Chem.* **1990**, *94*, 3373. (b) (HNP)$^+$ is preferred over (HPN)$^+$ by 68.7 kcal/mol at CISD/6-31G* and including the VZPEs determined at that level. (c) Buenker, R. J.; Bruna, P. J.; Peyerimhoff, S. D. *Isr. J. Chem.* **1980**, *19*, 309.

(24) Gaussian88: Frisch, M. J.; Head-Gordon, M.; Schlegel, H. B.; Raghavachari, K.; Binkley, J. S.; Gonzales, C.; Defrees, D. J.; Fox, D. J.; Whiteside, R. A.; Seeger, R.; Melius, C. F.; Baker, J.; Martin, R. L.; Kahn, L. R.; Stewart, J. J. P.; Fluder, E. M.; Topiol, S.; Pople, J. A. Gaussian, Inc., Pittsburgh, PA, 1988.

(25) Schlegel, H. B. *J. Comput. Chem.* **1982**, *3*, 214.

(26) Hehre, W. J.; Radom, L.; Schleyer, P. v. R.; Pople, J. A. *Ab Initio Molecular Orbital Theory*; John Wiley & Sons: New York, 1986.

(27) 6-31G* basis set: (a) Hehre, W. J.; Ditchfield, R.; Pople, J. A. *J. Chem. Phys.* **1972**, *56*, 2257. (b) Hariharan, P. C.; Pople, J. A. *Theor. Chim. Acta* **1973**, *28*, 213. (c) Binkley, J. S.; Gordon, J. S.; DeFress, D. J.; Pople, J. A. *J. Chem. Phys.* **1982**, *77*, 3654.

(28) (a) Binkley, J. S.; Pople, J. A. *Int. J. Quantum Chem.* **1975**, *9*, 229. (b) Pople, J. A.; Seeger, R. *Int. J. Quantum Chem.* **1976**, *10*, 1. (c) Pople, J. A.; Krishnan, R.; Schlegel, H. B.; Binkley, J. S. *Int. J. Quantum Chem.* **1978**, *14*, 91, 545. (d) Krishnan, R.; Frisch, M. J.; Pople, J. A. *J. Chem. Phys.* **1980**, *72*, 4244.

(29) (a) Krishnan, R.; Binkley, J. S.; Seeger, R.; Pople, J. A. *J. Chem. Phys.* **1980**, *72*, 650. (b) Five (seven) d (f) orbitals were used in conjunction with the valence-triple-$\zeta$ basis sets.
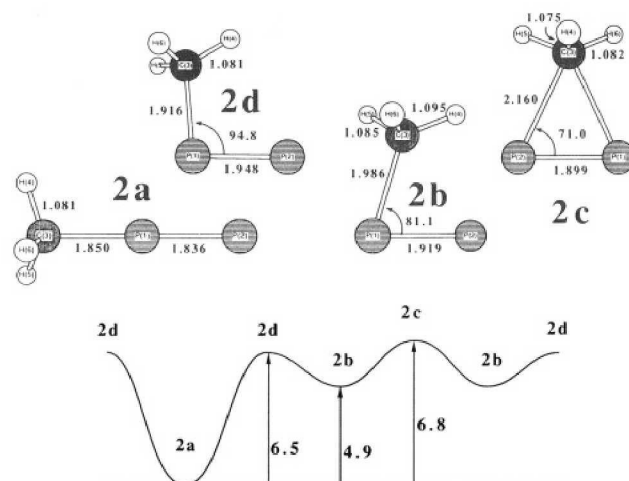
**Figure 1.** Schematic representation of the RHF potential energy surface of methyldiphosphonium cation. **2a** automerizes with small activation barriers via the intermediate **2b**.

Plesset perturbation theory in the frozen core approximation to full fourth order, MP4(sdtq), with the 6-31G* basis set and the RHF/6-31G* structures and also with the 6-311G(df,p) basis set and the MP2(full)/6-311G(df,p) structures. Electric polarizabilities were computed analytically at the RHF level and numerically as the dipole derivatives at the correlated levels.

Electronic structures were examined at the RHF/6-31G* and MP2(full)/6-31G* levels.[30] Topological and integrated properties were determined[31] with Extreme[32] and Proaim.[33,34] Natural populations were determined at the same level with the program NBO.[35] Cross sections of the electron densities were determined with Netz[36] and contoured with our PV Wave programs. Graphical representations of the atomic first moments were produced with our program Dipoles.[36]

## Results and Discussion

**Potential Energy Surfaces of the P Analogues of Diazonium Ions.** The potential energy surfaces of the methylated $P_2$ and PN molecules were first examined at the MP3/6-31G*//RHF/6-31G* level[37] to determine the most stable topologies of the molecules, which were then studied in more detail. For **1**, we had shown earlier that the $C_{3v}$ structure is the most stable one and that the symmetrically bridged structure is the transition state for automerization.[7]

**(a) Methyldiphosphonium Ion.** $C_{3v}$ **2a** is the global minimum (Figure 1). Structure $C_s$ **2b**, in which the $CH_3$ group coordinates $P_2$ in an asymmetric $\eta^2$ fashion, is a local minimum only 4.9 kcal/mol less stable than **2a**. Equilibrium between the two nonequivalent P atoms in **2b** is a facile process that requires only

(30) The correlated densities were calculated with Frisch's implementation of the Z-vector method. (a) Handy, N. C. and Schaefer, H. F., III *J. Chem. Phys.* **1984**, *81*, 5031. (b) See ref 24.

(31) After reformating with Psichk: (a) Lepage, T. J., Department of Chemistry, Yale University, 1988. (b) IBM version by Benjamin Harris, University of Missouri, Columbia, 1991.

(32) Extreme: (a) Biegler-König, F. W., McMaster University, Hamilton, ON, Canada, 1980. (b) Ported to the Silicon Graphics Personal Iris by the authors.

(33) Proaim: (a) Biegler-König, F. W.; Duke, F. A., McMaster University, Hamilton, ON, Canada, 1981. (b) Modifications by Lau, C. D. H., McMaster University, Hamilton, ON, Canada, 1983. (c) Ported to the Silicon Graphics Personal Iris by the authors.

(34) For details of the electron density integration algorithms, see: Biegler-König, F. W.; Bader, R. F. W.; Tang, T.-H. *J. Comput. Chem.* **1982**, *3*, 317.

(35) NBO 3.0: Glendening, E. D.; Reed, A. E.; Carpenter, J. E.; Weinhold, F., Theoretical Chemistry Institute and Department of Chemistry, University of Wisconsin, Madison, WI, 53706. (b) We thank Andy Holder for a copy of this program.

(36) Glaser, R., Department of Chemistry, University of Missouri—Columbia, 1990.

(37) RHF/6-31G* structures and MPx/6-31G* energies of the structures in Figures 1 and 2 are given as supplementary material.
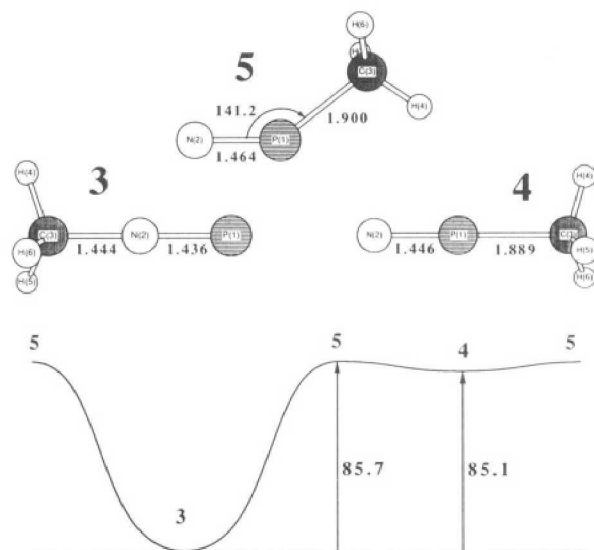
**Figure 2.** N methylation is preferred over P methylation for PN. At the RHF level, **4** corresponds to a very shallow minimum that easily interconverts to **3** via the transition-state structure **5**.



**Figure 3.** Molecular models of **1–4** as determined at the MP2(full)/6-311G(df,p) level. Structural parameters are given as determined at the levels RHF/6-31G*, MP2(fu)/6-311G*, MP2(fu)/6-311G**, and MP2(fu)/6-31G(df,p). Experimental values are given in italics.

1.9 kcal/mol, which is achieved by methyl rotation and translation via $C_s$ **2c** (a'' i237.7 cm$^{-1}$). The transition between **2a** and **2b** proceeds with retention of one of the symmetry planes of **2a** via **2d** (a' i110.0 cm$^{-1}$). The barriers for the isomerizations **2 → 2d → 2b** and **2b → 2d → 2a** are 6.5 and 1.5 kcal/mol, respectively. The MP3/6-31G*//RHF/6-31G* energies suggest that the characteristics of the potential energy surface are maintained. At this level, **2a** is more favored over the bridged structure **2b** by 5.6 kcal/mol and the barriers from **2a → 2b** and from **2b → 2a** are 12.1 and 0.3 kcal/mol, respectively. The results suggest that **2b** is less stable than **2a**, but the local minimum **2b** might disappear at the correlated level. We have therefore optimized a bridged structure of **2** also at the MP2(full)/6-31G* level without any symmetry constraints. The resulting structure is topologically equivalent to **2b**, and the bridging is slightly more symmetric.[38] At the MP2(full)/6-31G* level, this structure is 8.8 kcal/mol less stable than **2a**, and higher level MP$x$ calculations also indicate that **2b** remains less stable than **2a**.[38] These activation barriers are such that a $^{31}$P-NMR spectrum at normal temperature should show one signal at the average chemical shift of the P atoms in **2a**; two distinct signals should only be observable at low temperature.

**(b) Methylphosphoazonium and Methylazophosphonium Ions.** N as well as P methylation lead to $C_{3v}$ symmetric minima (Figure 2), but the former is thermodynamically much more favored (by 85.1 kcal/mol). P-Methylated **4** corresponds to a *very* shallow minimum and it easily isomerizes to **3** via **5**. At the MP3/6-31G*//RHF/6-31G* level, **4** is only 0.5 kcal/mol more stable than **5**, and it is 77.9 kcal/mol less stable than the N-methylated **3**.[39]

**(c) Protonation versus Methylation.** The potential energy surfaces of protonated N$_2$ and PN (vide supra) and of the methylated ions are qualitatively similar. In contrast, methylation of P$_2$ favors $C_{3v}$ **2a** while protonation prefers the bridged structure. Methylation and protonation result in qualitatively different

chemistries *in all cases* because the relative energies and, in particular, the proton and methyl cation affinities differ drastically.

**(d) Structural Flexibility.** For **1**, N scrambling requires complete dediazoniation, N$_2$ rotation, and reconnection. For the NP derivative, only $C_{3v}$ **3** is found to be stable while the P-methylated **4** is bonded, but marginally. In contrast, *all of the stationary structures of **2** are bonded with respect to CH$_3^+$ and P$_2$*. **2a–2d** all are more stable than the fragments (by at least 51.5 kcal/mol at MP3/6-31G*//RHF/6-31G*). Thus, scrambling of the P atoms in **2** is predicted to occur and to proceed via a tightly bound ion–molecule complex with comparatively low activation barriers.

**Properties of the Methylated Molecules. (a) Structures.** Energies and geometries of **1–4** are summarized in Table I and Figure 3. Model dependencies of the XY bonds in **1–4** and in the diatomic molecule follow the same trends, and similar trends had previously been reported for P$_2$[40-43] and PN.[44,45] Comparison with the experimental values for the diatomics[46,47] suggests that the

(38) (a) MP2(full)/6-31G* structure (C$_1$) of **2b**: P P, 1, 1.958 491; C, 1, 2.051 058, 2, 65.283; H, 3, 1.109 316, 1, 131.706, 2, 2.479, 0; H, 3, 1.089 933, 1, 99.171, 4, 119.684, 0; H, 3, 1.089 703, 1, 100.478, 4, -122.198, 0. (b) Energies in atomic units: MP2(full) = -721.089 364, MP2 = -721.061 485 5, MP3 = -721.088 909 1, MP4D = -721.101 698 3, MP4DQ = -721.090 681 9, MP4SDQ = -721.094 933 1, MP4SDTQ = -721.113 105 7. (c) Relative energies with regard to the MP2(fu)/6-31G* energy of **2a**, 8.81 kcal/mol. Relative energy with regard to **2a** at MP$x$(fc)/6-31G*//RHF/6-31G*: 5.93 (MP2), 4.07 (MP3), 5.14 (MP4(sdtq) kcal/mol.

(39) The RHF-PES of (MeNP)$^+$ makes it questionable whether **4** would survive as a minimum at higher levels or whether it would become the transition state for automerization of **3**. The MP2(full)/6-31G* frequency calculation for **4** indicates that it remains a minimum, and we note that the low-frequency mode is *higher* at this correlated level than at the RHF level.
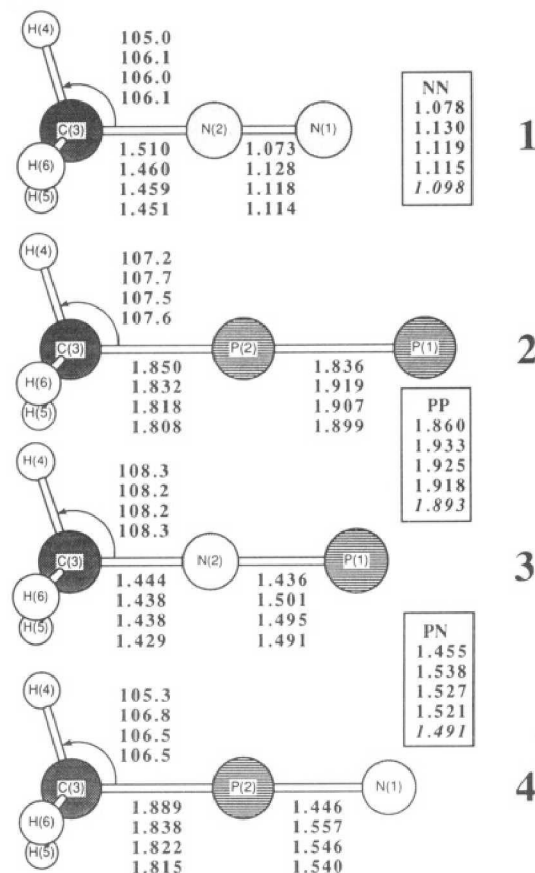
(40) Summary of prior theoretical studies of elemental P: Schmidt, M. W.; Gordon, M. S. *Inorg. Chem.* **1985**, *24*, 4503, and references therein.

(41) For near-HF-limit calculations of P$_2$, see: (a) Mulliken, R. S.; Liu, B. *J. Am. Chem. Soc.* **1971**, *93*, 6738. (b) CI calculations: McLean, A. D.; Liu, B.; Chandler, G. S. *J. Chem. Phys.* **1984**, *80*, 5130.

(42) Ab initio pseudopotential SCF calculations: (a) Osman, R.; Coffey, P.; Van Wazer, J. R. *Inorg. Chem.* **1976**, *17*, 287. (b) P$_n$ with *n* = 2, 4, 8: Trinquier, G.; Malrieu, J.-P.; Daudey, J.-P. *Chem. Phys. Lett.* **1981**, *80*, 552. (c) P$_2$ and P$_4$: Wedig, U.; Stoll, H.; Preuss, H. *Chem. Phys.* **1981**, *61*, 117.

(43) Brundle, C. R.; Kuebler, N. A.; Robin, M. B.; Basch, H. *Inorg. Chem.* **1972**, *11*, 20.

(44) For ab initio computations on PN and its protonated ions, see ref 23.

(45) A CI study of PN gave the correct equilibrium distance for the ground state: Grein, F.; Kapur, A. *J. Mol. Spectrosc.* **1983**, *99*, 25. Note that their CI energy is higher than the MP4 energies reported here.

(46) CRC *Handbook of Chemistry and Physics*, 63rd ed.; CRC Press: Boca Raton, FL, 1982/1983; p F-181.

(47) (a) Structure and frequency of P$_2$: Huber, K. P.; Herzberg, G. *Constants of Diatomic Molecules*; Van Nostrand Reinhold: New York, 1979. (b) Structure and frequency of PN: *Ibid.* p 564. (c) Structure and frequencies of N$_2$: *Ibid.* p 553.

**TABLE I: Total Energies and Vibrational Zero-Point Energies**[a-e]

| | | | energies | | | | |
|---|---|---|---|---|---|---|---|
| | | VZPE | RHF | MP2(full) | MP2(fc) | MP3 | MP4(sdtq) |
| A | (Me-NN)+ | 30.71 | -148.216 056 | | -148.645 851 | -148.653 683 | -148.682 754 |
| B | | 28.73 | -148.205 354 | -148.666 119 | | | |
| C | | | -148.246 336 | -148.784 934 | | | |
| D | | | -148.251 991 | -148.830 318 | -148.772 428 | -148.774 806 | -148.815 140 |
| A | (Me-PP)+ | 25.97 | -720.726 303 | | -721.070 933 | -721.095 388 | -721.121 305 |
| B | | 24.71 | -720.720 772 | -721.103 403 | | | |
| C | | | -720.769 160 | -721.421 708 | | | |
| D | | | -720.777 378 | -721.475 915 | -721.206 382 | -721.230 266 | -721.263 733 |
| A | (Me-NP)+ | 29.30 | -434.501 735 | | -434.898 437 | -434.908 846 | -434.940 697 |
| B | | 27.49 | -434.494 856 | -434.924 474 | | | |
| C | | | -434.539 629 | -435.143 369 | | | |
| D | | | -434.546 909 | -435.191 522 | -435.027 877 | -435.035 093 | -435.077 074 |
| A | (Me-PN)+ | 26.77 | -434.366 131 | | -434.788 395 | -434.785 475 | -434.833 406 |
| B | | 25.30 | -434.348 442 | -434.820 335 | | | |
| C | | | -434.393 598 | -435.038 875 | | | |
| D | | | -434.403 880 | -435.089 813 | -434.926 971 | -434.909 781 | -434.980 663 |
| A | Me+ | 21.16 | -39.230 640 | | -39.325 140 | -39.341 577 | -39.345 779 |
| B | | 20.40 | -39.230 412 | -39.329 435 | | | |
| C | | 20.11 | -39.243 501 | -39.374 322 | | | |
| D | | 20.14 | -39.243 770 | -39.384 074 | -39.365 605 | -39.384 990 | -39.389 933 |
| A | NN | 3.94 | -108.943 949 | | -109.248 190 | -109.245 335 | -109.266 487 |
| B | | 3.12 | -108.935 400 | -109.261 574 | | | |
| C | | 3.12 | -108.964 342 | -109.334 062 | | | |
| D | | 3.16 | -108.967 563 | -109.365 322 | -109.327 323 | 109.317 707 | -109.348 330 |
| A | PN | 2.27 | -395.125 750 | | -395.408 591 | -395.402 192 | -395.432 148 |
| B | | 1.65 | -395.116 449 | -395.430 212 | | | |
| C | | 1.69 | -395.149 679 | -395.600 123 | | | |
| D | | 1.72 | -395.154 491 | -395.634 350 | -395.490 833 | -395.476 510 | -395.518 530 |
| A | PP | 1.30 | -681.424 535 | | -681.638 749 | -681.652 396 | -681.656 504 |
| B | | 1.02 | -681.420 395 | -681.664 697 | | | |
| C | | 1.02 | -681.455 523 | -681.932 180 | | | |
| D | | 1.05 | -681.458 762 | -681.969 243 | -681.719 495 | -681.731 595 | -681.755 019 |

[a] Levels A–D are RHF/6-31G*, MP2(fu)/6-31G*, MP2(fu)/6-311G**, and MP2(fu)/6-311G(df,p), respectively. Six Cartesian d-type functions were used in the 6-31G* basis set. Five pure d-type orbitals were used in the 6-311G** basis sets. Seven pure f-type functions were used in the 6-311G(df,p) basis sets. [b] See Figure 3 for geometries. [c] Unscaled vibrational zero-point energies (VZPE) in kilocalories per mole. There were no negative eigenvalues in the analytically computed Hessian matrices. [d] Total energies in atomic units. [e] RHF and MP2(fu)/6-31G* results for $CH_3^+$, $N_2$, and 1 from ref 9. Note that the higher level energies reported in ref 9 all were based on the MP2(full)/6-31G* structures.

XY bond lengths are probably well bracketed by the RHF and the MP2/6-311G(df,p) results. The C–X bond lengths decrease as the theoretical model is improved. In the following, we will discuss the structures obtained at the highest level.[48] Methylation *shortens* the XY bond for the stable molecules 1–3, a result of the increased bond polarity (vide infra). The CN bond in 3 (1.491 Å) is somewhat shorter than the one in 1 (1.451 Å), as one might anticipate from the higher nucleophilicity of N in PN compared to $N_2$. The CP bond lengths in 2 and 4 are remarkably similar *although* 2 has a high methyl cation affinity whereas 4 does not. The PN bond in 3 (1.491 Å) is significantly shorter than the one in 4 (1.540 Å). The latter is comparable to the experimental PN bond length of 1.57 Å in PN+ in its $^2\Sigma^+$ state (formed by loss of the $7\sigma$ electron from PN).[49] The experimental bond lengths[50] of the $^2\Sigma^+$ (ground) states of $N_2^+$ (1.116 Å) and $P_2^+$ (1.893 Å) are very close to the values in the neutral molecules, and thus, they may not be taken as an indicator of the charge distribution in 1 and 2. The HCX angles are little susceptible to the theoretical model, and they all are *rather similar* (106–108.5°) *no matter what the methyl cation affinity is*. Clearly, to understand the "CX bond strengths" the "XY bonds" need to be considered.

(b) **Methyl Cation Affinities.** Electron correlation greatly *increases* the affinities (Table II). Basis set improvements at the correlated level yield affinities that are generally higher by 4–8 kcal/mol, and in particular, the two sets of MP4(sdtq) affinities differ by up to 11 kcal/mol. The MP4(sdtq)/6-311G(df,p)//

MP2(full)/6-311G(df,p) affinities will be discussed. Better correlation treatments and even larger basis sets might still affect the affinities, but these changes (probably within 5 kcal/mol) are not expected to affect our conclusions.

P substitution of $N_\beta$ *dramatically increases* the MCA (to 105.8 kcal/mol) whereas P substitution of $N_\alpha$ results in only a *modest decrease* (to 45.3 kcal/mol[51]). *Methylation of NP greatly favors methylphosphoazonium ions 3 and not 4*. An MCA of 74.5 kcal/mol is predicted for $P_2$, about midway between those of $N_2$ and NP. Both *the affinities of $P_2$ and of NP are predicted to be significantly higher than that of $N_2$*, suggesting that 2 and 3 should be stable molecules in the gas phase. These MCAs are lowered by the changes in the vibrational zero-point energies (VZPEs) upon methylation, which were estimated at the RHF/6-31G* and MP2/6-31G* levels (Table II). The data for diatomic molecules[52] suggest that the MP2/6-31G* VZPEs are somewhat overestimated, but those effects should nearly cancel for the ΔVZPEs. With the MP2/6-31G* ΔVZPE values, we report our best estimates for the binding energies of 1–4 to be 43.03, 71.3, 100.4, and 42.1 kcal/mol, respectively.

(c) **$P_2$ Dimerization.** Cations 2 might provide for a new way of stabilizing $P_2$. The dimerization of $P_2$ is relevant because it reduces the thermodynamic stability of 2 with regard to C–P dissociation and because it plays a role in the possible synthesis of 2 by alkylation of phosphorus. Reaction of carbenium ion

(48) Note that the geometry of 3 closely resembles that observed for the *aryl* derivative reported by Niecke et al. (PN = 1.493 Å and CN = 1.397 Å); see refs 5 and 6.

(49) (a) Obase, H.; Tsuji, M.; Nishimura, Y. *Chem. Phys. Lett.* **1981**, *81*, 119. (b) Obase, H.; Tsuji, M.; Nishimura, Y. *Chem. Phys.* **1983**, *74*, 89.

(50) For a comparison of $N_2^+$, PN+ and $P_2^+$, see: Grein, F. *Chem. Phys.* **1988**, *120*, 383.

(51) Note that 4 is predicted to be strongly bonded in contrast to the RHF/6-31G* level.

(52) The vibrational frequencies of $N_2$, PN, and $P_2$ are 2359.6 ($^1\Sigma_g^+$), 1337.0 ($^1\Sigma^+$), and 780.8 cm$^{-1}$ ($^1\Sigma_g^+$), respectively. The scale factors necessary to match the computed with the experimental values are given (levels A–D) for $N_2$, 0.86, 1.08, 1.08, and 1.07, for PN, 0.84, 1.16, 1.13, and 1.11, and for $P_2$, 0.86, 1.09, 1.09, and 1.06, respectively. The RHF frequencies are severely *over*estimated while they are *under*estimated at the correlated level.

**TABLE II: Methyl Cation Affinities**[a-c]

| | RHF | MP2(full) | MP2(fc) | MP3 | MP4(sdtq) | ΔVZPE |
|---|---|---|---|---|---|---|
| | | | (Me-NN)+ (1) | | | |
| RHF/6-31G* | 26.02 | | 45.51 | 41.90 | 44.23 | -5.61 |
| MP2(fu)/6-31G* | 24.81 | 47.13 | | | | -5.21 |
| MP2(fu)/6-311G** | 24.15 | 48.04 | | | | |
| MP2(fu)/6-311G(df,p) | 25.51 | 50.78 | 49.89 | 45.25 | 48.24 | |
| | | | (Me-PP)+ (2) | | | |
| RHF/6-31G* | 44.63 | | 67.17 | 63.64 | 74.69 | -3.51 |
| MP2(fu)/6-31G* | 43.90 | 68.57 | | | | -3.29 |
| MP2(fu)/6-311G** | 44.01 | 79.29 | | | | |
| MP2(fu)/6-311G(df,p) | 46.97 | 76.93 | 76.11 | 71.34 | 74.54 | |
| | | | (Me-NP)+ (3) | | | |
| RHF/6-31G* | 91.21 | | 103.35 | 103.59 | 102.14 | -5.87 |
| MP2(fu)/6-31G* | 92.87 | 103.43 | | | | -5.44 |
| MP2(fu)/6-311G** | 91.90 | 106.00 | | | | |
| MP2(fu)/6-311G(df,p) | 93.28 | 108.62 | 107.58 | 108.93 | 105.81 | |
| | | | (Me-PN)+ (4) | | | |
| RHF/6-31G* | 6.11 | | 34.30 | 26.17 | 34.81 | -3.34 |
| MP2(fu)/6-31G* | 0.99 | 38.08 | | | | -3.25 |
| MP2(fu)/6-311G** | 0.26 | 40.43 | | | | |
| MP2(fu)/6-311G(df,p) | 3.53 | 44.80 | 44.26 | 30.30 | 45.31 | |

[a] Reaction energies for $RXY^+ \rightarrow R^+ + XY$ in kilocalories per mole. [b] $\Delta VZPE = VZPE(Me^+) + VZPE(XY) - VZPE(MeXY^+)$. $\Delta VZPE$ is given in kilocalories per mole and unscaled. These values give the reduction of the binding energies. [c] See footnote e of Table I.

**TABLE III: Properties of the Methyl Compounds**[a]

| parameter | (MeNN)+ (1) | (MePP)+ (2) | (MeNP)+ (3) | (MePN)+ (4) |
|---|---|---|---|---|
| dipole $\mu$ | 3.613 | 8.364 | 8.564 | 3.876 |
| quadrupole $\theta_{perp}$ | -14.444 | -28.991 | -21.130 | -20.962 |
| quadrupole $\theta_{para}$ | -7.718 | 1.220 | 6.045 | -16.168 |
| polarizability $\alpha_{perp}$ | 14.473 | 29.087 | 22.027 | 21.206 |
| polarizability $\alpha_{para}$ | 27.827 | 83.348 | 51.312 | 54.020 |
| rotational constant | 152.019 | 154.193 | 155.390 | 152.202 |
| rotational constant | 9.482 | 3.210 | 5.246 | 5.652 |

[a] At MP2(full)/6-31G*. Dipole moments in debye (1 au = 2.5418 D), quadrupoles in debye angstroms. Polarizabilities in atomic units, and rotational constants in gigahertz.

sources with white phosphorus ($P_4$) would presumably involve initial formation of tetraphosphonium ions. Stabilization of $P_2$ in **2** would be possible if the stability of **2** were to overcompensate for $P_4$ fragmentation.[53] Experimental $P_2$ dimerization enthalpies were determined by two independent methods,[54-56] and this dimerization reduces the binding energy of **2** with regard to $CH_3^+$ and $P_4$ by ~27 kcal/mol. Nevertheless, the reaction $CH_3^+ + 0.5P_4 \rightarrow$ **2** remains exothermic by 44 kcal/mol, and even with the dimerization of $P_2$ considered, the P analogues **2** should be just as stable toward demethylation as are the diazonium ions.

**(d) PN Expulsion and Phosphaazene Formation.** As with $P_2$, PN has comparatively weak $\pi$ bonds and shows a tendency toward polymerization, thereby reducing the thermodynamic stability

(53) Another requirement is that the methyl cation affinity of $P_2$ overcompensates for the methyl cation affinity of $P_4$ and the $P_2$ dimerization energy. Preliminary studies show this to be the case (to be published).

(54) (a) The determination of the equilibrium constant of the reaction $P_4(g) \rightarrow 2P_2(g)$ by Farr gave a value of 54.6 kcal/mol: National Bureau of Standards. *JANAF Thermochemical Tables*, 2nd ed.; NSRDS-NB 37; U.S. Department of Commerce, U.S. Government Printing Office: Washington, DC, 1971. (b) This value was confirmed by photoelectron spectroscopic measurements of the $T$ dependence of the equilibrium constant ($\Delta H° = 55$ kcal/mol): Bock, H.; Müller, H. *Inorg. Chem.* **1984**, *23*, 4365.

(55) The threshold of 12.85 eV for the mass spectroscopic formation of $P_2^+$: Drowart, J.; Smets, J.; Reynaert, J. C.; Coppens, P. *Adv. Mass Spectrom.* **1978**, *7A*, 647. Note that the dimerization energy of 54.9 kcal/mol reported there is slightly off because the ionization potential of the P atom instead of that of $P_2$ was used and the ionization potential of $P_2(g)$ of 10.57 eV (Carroll, P. K.; Mitchell, P. I. *Proc. R. Soc. London A* **1975**, *342*, 93) results in a value of 52.6 kcal/mol. Consideration of the more recent value of 12.91 eV for $P_4$ + $e^- \rightarrow P_2^+ + P_2 + 2e^-$ (Monnom, G.; Gaucherel, Ph.; Paparoditis, C. *J. Phys.* **1984**, *45*, 77) results in $\Delta H° = 54.0$ kcal/mol.

(56) Ahlrichs, R.; Brode, S.; Ehrhardt, C. *J. Am. Chem. Soc.* **1985**, *105*, 7260.

**TABLE IV: Vibrational Spectroscopic Properties of the Methyldiazonium Analogues**[a]

| molecule | $\nu_{calc}$ | | $m_{red}$ | $f$ | IR intensity |
|---|---|---|---|---|---|
| (MeNN)+ | 346.6 | e | 4.750 | 0.336 | 0.33 |
| | 767.5 | a₁ | 7.566 | 2.626 | 6.51 |
| | 1168.2 | e | 1.332 | 1.071 | 0.84 |
| | 1464.3 | a₁ | 1.130 | 1.427 | 9.09 |
| | 1489.9 | e | 1.037 | 1.356 | 33.59 |
| | 2218.9 | a₁ | 12.929 | 37.503 | 4.78 |
| | 3122.7 | a₁ | 1.024 | 5.884 | 36.08 |
| | 3257.4 | e | 1.112 | 6.953 | 42.67 |
| (MePP)+ | 62.2 | e | 6.034 | 0.014 | 3.86 |
| | 530.1 | a₁ | 6.844 | 1.133 | 1.08 |
| | 837.6 | a₁ | 17.857 | 7.382 | 4.55 |
| | 947.4 | e | 1.185 | 0.627 | 0.70 |
| | 1374.8 | a₁ | 1.139 | 1.268 | 0.18 |
| | 1472.3 | e | 1.050 | 1.342 | 29.03 |
| | 3110.1 | a₁ | 1.027 | 5.851 | 45.50 |
| | 3237.0 | e | 1.109 | 6.843 | 26.63 |
| (MePP)+ | 311.0 | e | 4.333 | 0.247 | 17.46 |
| | 737.0 | a₁ | 6.316 | 2.021 | 2.93 |
| | 1150.5 | e | 1.328 | 1.035 | 0.22 |
| | 1450.5 | a₁ | 2.136 | 2.648 | 5.37 |
| | 1504.9 | e | 1.037 | 1.384 | 27.92 |
| | 1518.5 | a₁ | 2.118 | 2.878 | 0.83 |
| | 3118.1 | a₁ | 1.028 | 5.887 | 24.70 |
| | 3236.5 | e | 1.108 | 6.841 | 10.95 |
| (MePP)+ | 145.5 | e | 6.592 | 0.082 | 2.13 |
| | 582.7 | a₁ | 6.317 | 1.264 | 0.44 |
| | 966.8 | e | 1.195 | 0.658 | 5.36 |
| | 1067.2 | a₁ | 16.983 | 11.395 | 90.18 |
| | 1367.5 | a₁ | 1.138 | 1.254 | 0.31 |
| | 1458.6 | e | 1.050 | 1.367 | 28.69 |
| | 3089.7 | a₁ | 1.025 | 5.764 | 47.17 |
| | 3224.6 | e | 1.111 | 6.803 | 50.54 |

[a] MP2(full)/6-31G*. Frequencies in reciprocal centimeters, force constants in millidynes per angstrom, and IR intensities.

of **3**. To estimate the effect of such polymerization, the cyclic benzene analogue PN trimer
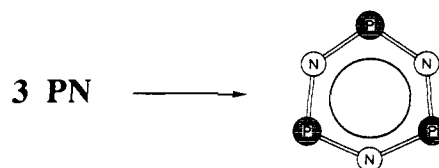


$D_{3h}$ (PN)$_3$ was optimized at RHF/6-31G* and energies were

**TABLE V: Topological Properties[a]**

|   | bond | $r_A$ | $r_B$ | $F$ | $\rho$ | $\lambda_1$ | $\lambda_2$ | $\lambda_3$ | $\epsilon$ |
|---|------|-------|-------|-----|--------|-------------|-------------|-------------|------------|
| | | | | $(MeNN)^+$ (1)[b] | | | | | |
| A | C–H | 0.728 | 0.350 | 0.675 | 0.294 | −0.873 | −0.837 | 0.490 | 0.044 |
| A | C–N | 0.457 | 1.053 | 0.302 | 0.171 | −0.083 | −0.083 | 0.762 | 0.000 |
| A | N–N | 0.586 | 0.487 | 0.546 | 0.690 | −1.560 | −1.560 | 0.491 | 0.000 |
| B | C–H | 0.740 | 0.352 | 0.678 | 0.277 | −0.805 | −0.776 | 0.509 | 0.038 |
| B | C–N | 0.458 | 1.002 | 0.314 | 0.204 | −0.189 | −0.189 | 0.720 | 0.000 |
| B | N–N | 0.604 | 0.523 | 0.536 | 0.592 | −1.281 | −1.281 | 0.865 | 0.000 |
| | | | | $(MePP)^+$ (2) | | | | | |
| A | C–H | 0.717 | 0.364 | 0.663 | 0.284 | −0.800 | −0.783 | 0.477 | 0.021 |
| A | C–P | 0.878 | 0.982 | 0.472 | 0.160 | −0.215 | −0.215 | 0.099 | 0.000 |
| A | P–P | 1.166 | 0.670 | 0.635 | 0.157 | −0.092 | −0.092 | 0.537 | 0.000 |
| B | C–H | 0.729 | 0.363 | 0.668 | 0.270 | −0.749 | −0.737 | 0.500 | 0.016 |
| B | C–P | 0.993 | 0.838 | 0.542 | 0.156 | −0.190 | −0.190 | 0.040 | 0.000 |
| B | P–P | 1.197 | 0.719 | 0.624 | 0.142 | −0.080 | −0.080 | 0.197 | 0.000 |
| | | | | $(MeNP)^+$ (3) | | | | | |
| A | C–H | 0.710 | 0.370 | 0.658 | 0.289 | −0.826 | −0.793 | 0.490 | 0.041 |
| A | C–N | 0.448 | 0.996 | 0.310 | 0.231 | −0.341 | −0.341 | 0.840 | 0.000 |
| A | N–P | 0.852 | 0.584 | 0.593 | 0.238 | −0.382 | −0.382 | 2.900 | 0.000 |
| B | C–H | 0.727 | 0.364 | 0.666 | 0.275 | −0.778 | −0.752 | 0.512 | 0.035 |
| B | C–N | 0.467 | 0.971 | 0.325 | 0.239 | −0.348 | −0.348 | 0.552 | 0.000 |
| B | N–P | 0.898 | 0.603 | 0.598 | 0.206 | −0.302 | −0.302 | 2.150 | 0.000 |
| | | | | $(MePN)^+$ (4) | | | | | |
| A | C–H | 0.729 | 0.353 | 0.674 | 0.286 | −0.826 | −0.805 | 0.478 | 0.027 |
| A | C–P | 0.812 | 1.077 | 0.430 | 0.143 | −0.182 | −0.182 | 0.146 | 0.000 |
| A | P–N | 0.586 | 0.860 | 0.405 | 0.247 | −0.320 | −0.320 | 2.589 | 0.000 |
| B | C–H | 0.736 | 0.358 | 0.673' | 0.269 | −0.753 | −0.740 | 0.498 | 0.017 |
| B | C–P | 0.934 | 0.904 | 0.508 | 0.154 | −0.192 | −0.192 | 0.080 | 0.000 |
| B | P–N | 0.626 | 0.931 | 0.402 | 0.192 | −0.193 | −0.193 | 1.313 | 0.000 |

[a] A "B" indicates RHF/6-31G* (MP2(fu)/6-31G*) density. $r_A$ and $r_B$ are the distances of atoms A and B from the bond critical points in angstroms, $F$ is defined as $F = r_A/(r_A + r_B)$, $\rho$ is the electron density at the critical point in e au$^{-3}$, the $\lambda_i$ are the principal curvatures in the density in e au$^{-5}$, and $\epsilon$ is the bond ellipticity. [b] RHF/6-31G* values for 1 from ref 7, and MP2/6-31G* values for 1 from ref 9.

determined up to the MP3(fc)/6-31G* level with the RHF geometry.[57] At the MP3 level, the energy for the reaction 3PN → $D_{3h}$ (PN)$_3$ is 59.0 kcal/mol. Thus, polymerization of PN reduces the energy of the dissociation reaction 3 → $CH_3^+$ + $^1/_3(PN)_3$ only by ~19.7 kcal/mol.

**(e) Spectroscopic Properties.** The thermodynamic stabilities of 2 and 3 are such that they might be detectable in the gas phase. Pertinent properties are listed in Table III, vibrational data are summarized in Table IV, and the IR spectra (MP2(full)/6-31G*) of 2–4 are shown in Figure 4. The IR spectra differ characteristically in the region below 1500 cm$^{-1}$. All ions show a signal at ~1500 cm$^{-1}$ for CH$_3$ bending modes. For 2, this CH$_3$ bending is the only significant band in that region. Weak signals, corresponding to CX and XY stretching modes, occur at 838 cm$^{-1}$ for 2 and at 737 cm$^{-1}$ for 3. 3 exhibits several additional diagnostic signals including a weak band at 1451 cm$^{-1}$ (CH$_3$ umbrella mode, not visible in 2 and 4) and a signal at 311 cm$^{-1}$ (CNP angle deformation). The spectrum of 4 is characterized by the strong signal at 1067 cm$^{-1}$ (mostly NP stretching). Considering the relative energies of 3 and 4, the *absence* of this signal might be of diagnostic value.

**Electronic Structures. (a) Topological Analysis.** Topological and integrated properties of 1–4 are summarized in Tables V and VI, respectively. The inclusion of electron correlation has significant effects on these properties. For example, the CH$_3$ populations are larger at the correlated level. However, this finding alone cannot be taken as an indication that the charge transfer from XY to the CH$_3$ group is increased by electron correlation. *These significant changes in the numbers derived from the topological analysis do not necessarily reflect large changes in the electron density distributions themselves.* In our previous study of methyl- and ethyldiazonium ions,[9] we analyzed correlation effects carefully. Major electron correlation effects were found primarily in the core regions, and comparatively small effects
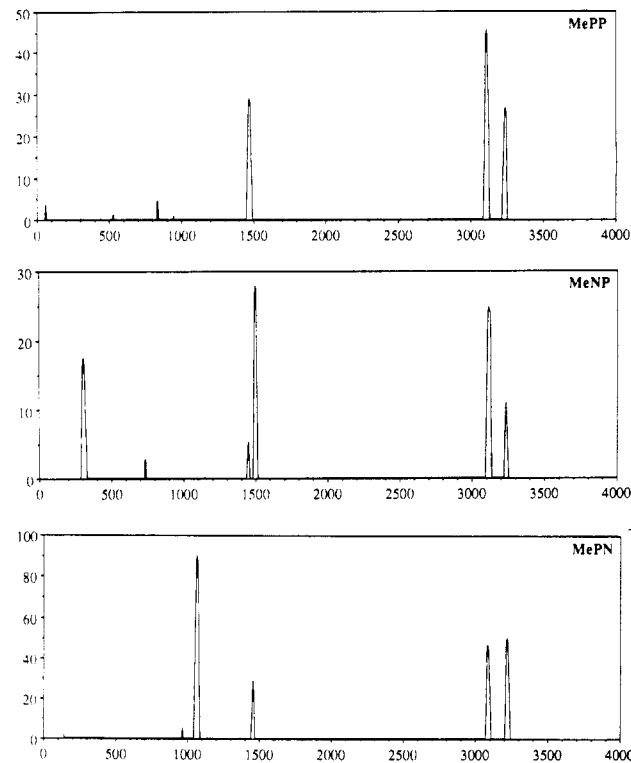
(57) $D_{3h}$ (PN)$_3$ (X is the ring center): PX = 1.6831 Å, NX = 1.5195 Å, PN = 1.6076 Å, $E$(RHF/6-31G*) = −1185.498 448 hartrees, $E$(MP2(fc)/6-31G*) = −1186.294 292 hartrees, $E$(MP3) = −1186.300 609 hartrees.



Figure 4. Infrared spectra of 2–4 as computed at the MP2(full)/6-31G* level.

occurred in the bonding regions. But even these small changes in the bonding regions may cause large changes on the derived properties because of the way the atomic populations are defined via the zero-flux surfaces. The point is well made by consideration of the critical features in the C–X bonding regions. Since we are comparing molecules with different CX bond lengths, we are using the relative $F$ values. The $F_{CX}$ value in 1 is ~0.3; that is, the C

**TABLE VI: Atomic Properties**

| | RHF | | | | MP2 | | | |
|---|---|---|---|---|---|---|---|---|
| | NC[a] | IBP[b] | $\mu^c$ | $T^d$ | NC[a] | IBP[b] | $\mu^c$ | $T^d$ |
| **1**[e] | | | | | | | | |
| H | 0.305 | 0.808 | 0.123 | 0.538 80 | 0.328 | 0.783 | 0.131 | 0.516 51 |
| C | −0.418 | 5.736 | 0.653 | 37.718 47 | −0.531 | 5.821 | 0.635 | 37.743 71 |
| X(C) | 0.096 | 7.397 | 0.335 | 54.877 29 | 0.187 | 7.256 | 0.384 | 54.722 32 |
| Y(X) | 0.407 | 6.443 | 0.717 | 54.003 88 | 0.361 | 6.575 | 0.706 | 54.065 39 |
| Σ | | 22.000 | | 148.216 03 | | 22.001 | | |
| CH₃ | 0.497 | 8.160 | | 39.334 86 | 0.453 | 8.170 | | |
| **2** | | | | | | | | |
| H | 0.313 | 0.844 | 0.129 | 0.545 93 | 0.325 | 0.820 | 0.140 | 0.530 12 |
| C | −0.896 | 6.254 | 0.059 | 37.831 17 | −0.961 | 6.494 | 0.286 | 38.077 34 |
| X(C) | 0.472 | 15.418 | 2.141 | 341.466 60 | 0.536 | 14.880 | 1.645 | 340.690 57 |
| Y(X) | 0.484 | 13.795 | 1.426 | 339.780 72 | 0.450 | 14.167 | 0.916 | 340.233 93 |
| Σ | | 37.999 | | 720.716 29 | | 38.001 | | |
| CH₃ | 0.043 | 8.786 | | 39.468 97 | 0.014 | 8.954 | | |
| **3**[f] | | | | | | | | |
| H | 0.276 | 0.883 | 0.130 | 0.571 57 | 0.300 | 0.838 | 0.140 | 0.543 50 |
| C | −0.437 | 5.577 | 0.671 | 37.542 98 | −0.520 | 5.746 | 0.660 | 37.708 52 |
| X(C) | −0.911 | 8.769 | 1.140 | 55.282 87 | −0.640 | 8.384 | 0.916 | 55.182 10 |
| Y(X) | 1.519 | 13.004 | 1.780 | 339.957 63 | 1.260 | 13.359 | 1.567 | 339.823 62 |
| Σ | | 29.999 | | 434.498 18 | | 30.003 | | |
| CH₃ | 0.391 | 8.226 | | 39.257 68 | 0.380 | 8.260 | | |
| **4** | | | | | | | | |
| H | 0.329 | 0.801 | 0.126 | 0.526 73 | 0.340 | 0.792 | 0.134 | 0.516 39 |
| C | −0.857 | 6.170 | 0.106 | 37.839 95 | −0.985 | 6.438 | 0.153 | 38.053 40 |
| X(C) | 1.505 | 13.045 | 1.305 | 340.153 54 | 1.350 | 13.401 | 0.654 | 340.027 03 |
| Y(X) | −0.634 | 8.384 | 1.411 | 54.791 71 | −0.385 | 7.787 | 0.746 | 54.677 60 |
| Σ | | 30.002 | | 434.366 13 | | 30.002 | | |
| CH₃ | 0.130 | 8.573 | | 39.420 14 | 0.035 | 8.814 | | |

[a] Natural charges. [b] Integrated atom populations. [c] Integrated atomic first moments in atomic units. [d] Integrated atomic kinetic energy $T$. $T$ values reported for the RHF level are corrected for the virial defects of the wave functions. [e] RHF and MP2 values for **1** from refs 7 and 9, respectively. [f] For comparison, the values for PN are NC(N) = −0.878 (RHF) and NC(N) = −0.694 (MP2).

basin covers about one-third of the CX-bonding region. At the correlated level, the $F_{CX}$ values all are increased—comparatively little for the CN bonds (0.012 for **1** and 0.015 for **3**) and more for the CP bonds (0.070 for **2** and 0.078 for **4**). Part of the increase of the CH₃ populations results from the increase in the C basin in the CX-bonding region. To correctly appreciate the effects of electron correlation, it becomes imperative to consider the populations with reference to the changes in the basins. The atomic moment[58] is a parameter that lends itself perfectly to assessment of the changes in the basins as it reflects the changes in the zero-flux surfaces defining each atom in the molecule. The combined consideration of the atomic populations *and* of the dipole moments should allow for a better appreciation of the correlation effects on the electron density distributions as the latter provide a measure for volume changes of the basins. The $\mu$ vectors (Table VI) are displayed in Figure 5 for **2–4**.[59] The absolute values are given in atomic units (1 au = 2.5418 D). The exact angles enclosed between the $\mu$ vectors and the bond directions were determined, and they were found to be negligibly small. In the following, we will discuss the values derived at the correlated level unless otherwise noted.

**(b) Populations.** The integrated CH₃ charges of **1–4** are +0.83, +0.05, +0.74, and +0.19, respectively. As with **1**, most of the + charge of **3** is located on the hydrocarbon fragment. In sharp contrast, the molecules with CP bonds have moderate to small CH₃ charges. The determination of the charge distribution within the XY fragment crucially depends on the zero-flux surface in that bonding region. The smaller the gradient $\lambda_3$ is in that region, the less significant arguments become regarding this internal polarization since very small effects may displace the zero-flux surface and cause large changes in the integrated properties. **3**
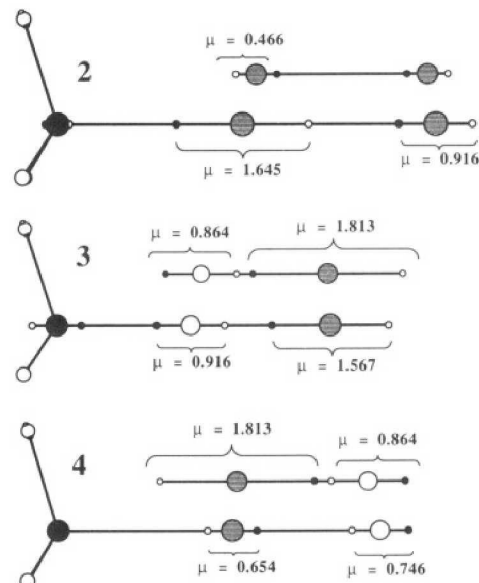


**Figure 5.** Integrated atomic dipole moments (au) as determined with the MP2(full)/6-31G* electron densities of **2–4** and of the diatomics. The $\mu$ vectors (O—●) are superimposed on the molecules and they are directed from the unfilled O to the filled ● markers.

has the largest $\lambda_3$ value for the XY bond and a strong polarization in the sense (−)N–P(+) is clearly indicated, but its magnitude depends greatly on the theoretical model. At least qualitatively, it can be concluded that the diazonium ion and its $P_\beta$ analogue show a common pattern: The $\beta$ substitution primarily serves to increase the internal XY polarization but has little effect on the overall charge transfer from the XY fragment to the CH₃ group. We had argued earlier that the electrostatic contributions to the CN bond strength in **1** caused by the CH₃-charge XY-dipole interaction are important, and the results for **3** suggest that the same is true in this molecule where the P substitution assists in increasing the internal polarization. P substitution in the $\alpha$ position

---

(58) The atomic moment $\mu$ is defined as the negative of the volume integral of $r' \rho(r)$ over the basin, where $r'$ measures the distance of the position $r$ from the position of the nucleus $Y$ ($r' = r − Y$).

(59) The atomic dipole moments (au) of $P_2$ and PN at MP2(full)/6-31G* P in $P_2$, −0.466; P and N in PN, −1.813 and −0.864, respectively. See Figure 5. The N charge in PN is −1.233. Note that the dipole moment of $P_2$ was determined via a "natural partitioning" into two P basins, which partitions the nonnuclear attractor in the $P_2$ bond equally.

**TABLE VII: Electron-Transfer Energies (kcal/mol)[a]**

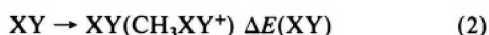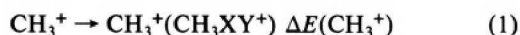| molecule | $\Delta E(CH_3^+)$ | $\Delta E(XY)$ | $\Delta E_{pro}$ |
|---|---|---|---|
| 1 | 20.56 | 0.01 | 67.70 |
| 2 | 24.74 | 0.09 | 93.39 |
| 3 | 26.33 | 0.71 | 130.47 |
| 4 | 22.41 | 0.23 | 60.72 |

[a] At MP2(full)/6-31G*.

or of both of the N atoms changes the bonding pattern dramatically. Significant charge transfer to the $CH_3$ group occurs, and with it perishes the incentive for internal $(-)XY(+)$ polarization. In **4**, the XY polarity is reversed (to the one expected on the basis of electronegativity). In **2**, both of the P atoms carry significant positive charges and the quantitative assignments of P charges is impeded by the characteristics of the PP-bonding region.

**(c) Atomic Dipole Moments.** In $P_2$, the $\mu$ vectors point to the center of the molecule. Formation of **2** increases both moments, and $\mu(P_\beta)$ is reversed. The shift of the zero-flux surface in the PP region toward $P_\beta$ tends to increase $\mu(P_\beta)$ and reduce $\mu(P_\alpha)$. Another reason for the $\mu(P_\alpha)$ reduction is the density depletion in the CP-bonding region, and the change in the direction of $\mu(P_\alpha)$ indicates this effect to be pronounced. PN is polar, and the bond critical point occurs closer to P than to N ($F_{NP} = 0.61$) causing $\mu(P)$ to point toward N but $\mu(N)$ to be parallel. Formation of **3** reduces $F_{NP}$, and both dipole moments are reduced while maintaining their direction. Formation of **4** changes $F_{NP}$ to about the same extent, but in this case, $\mu(P)$ is reduced much more because of the depletion in its basin in the CP-bonding region. The changes in the dipole moments of the $\beta$ heteroatom can thus all be rationalized by considering the $F_{XY}$ values, and changes of the $\alpha$ heteroatoms additionally reflect the degree of electron depletion in the $X_\alpha$ basin in the CX-bonding regions. For **2** and **4**, the latter are large and for **3** they are small. The $\mu(C)$ vectors also are characteristically different for **2** and **4** compared to **1** and **3**. In CN bonds, the $\mu(C)$ vector points toward $X_\alpha$ while it points in the opposite direction in CP bonds. These changes correlate inversely with the $CH_3$ charge. The more cationic the $CH_3$ carbon, the more its electron density is polarized away from the XY fragment.

It is one of the advantages of real-space electron density analysis that the high *anisotropy of the atomic basins*, manifested in the topological bond properties and quantified by the atomic first moments, *clearly comes to the fore*. Other partitioning methods result only in populations, and the partitioning cannot be traced easily. We determined the natural charges of **1–4** (Table VI). The most striking difference occurs for C in that the natural populations are much larger than the integrated populations. The natural populations of the H atoms consistently are lower than the integrated values, but smaller positive charges are predicted for the $CH_3$ groups nevertheless. These differences are largest for **1** and **3** with their high C–N polarity, and they affect the $X_\alpha$ populations inversely. The natural population analysis underestimates the C–$X_\alpha$ polarity, and it does not reflect the electron density accumulation at $X_\alpha$ sufficiently, which is clearly indicated by the integrated populations and well supported by the analysis of electron density difference functions.

**Electron Density Difference Functions and Charge-Transfer Energies.** The electronic and the energetic relaxations upon methylation consist of effects caused by the structural changes *within* the fragments (eqs 1 and 2) and of effects associated with

$$CH_3^+ \rightarrow CH_3^+(CH_3XY^+) \quad \Delta E(CH_3^+) \qquad (1)$$

$$XY \rightarrow XY(CH_3XY^+) \quad \Delta E(XY) \qquad (2)$$

$$CH_3^+(CH_3XY^+) + XY(CH_3XY^+) \rightarrow CH_3XY^+ \quad \Delta E_{pro} \qquad (3)$$

$$CH_3^+ + XY \rightarrow CH_3XY^+ \quad MCA \qquad (4)$$

the charge transfer between these "profragments" (eq 3).[60] In
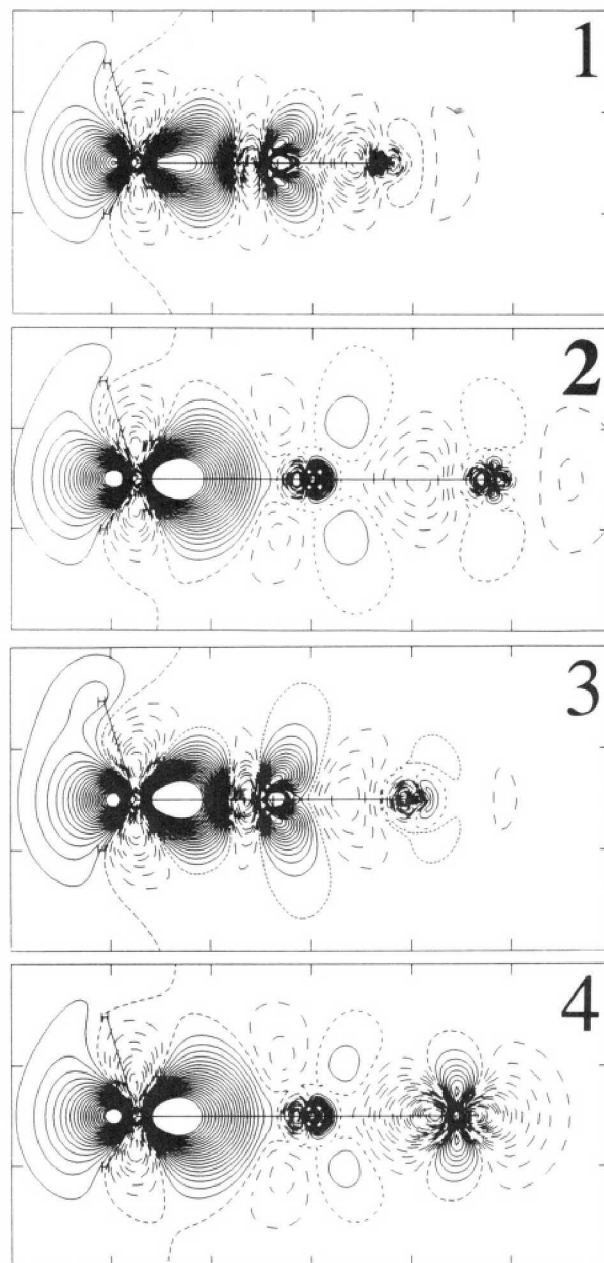


**Figure 6.** Electronic relaxation upon C–X bond formation. Contour plots are shown of the MP2(full)/6-31G* electron density difference functions $\Delta\rho = \rho(CH_3XY^+) - \rho^M(CH_3^+) - \rho^M(XY)$ for the ions **1–4**. Solid (dashed) lines indicate positive (negative) regions in $\Delta\rho$. Contours range from $-0.1$ to $0.1$ e au$^{-3}$ with a spacing of 0.005 e au$^{-3}$.

these equations, the notation $XY(CH_3XY^+)$, for example, refers to the *free* molecule XY with the geometry XY assumes in the molecule specified in parentheses. The electronic changes associated with the combination of the profragments are illustrated in a compelling fashion by the electron density difference function $\Delta\rho = \rho(MeXY^+) - \rho^M(CH_3^+) - \rho^M(XY)$. The superscript M in $\rho^M(CH_3^+)$ and $\rho^M(XY)$ indicates that the electron density functions of the fragments $CH_3^+$ and XY were determined with their geometries in **1–4**. The reaction energies of the steps of the methylations were evaluated at the MP2(full)/6-31G* level (Table VII) and the $\Delta\rho$ functions are displayed in Figure 6 with common contour level settings.

Structural changes in the XY fragments have negligible effects—the $\Delta E(XY)$ values are less than 0.7 kcal/mol. The

(60) It is emphasized that this analysis differs fundamentally from the one we have described earlier (ref 9). The fragment energy analysis described there relies on the integrated kinetic energies of the fragments *in* the molecules that are determined at the RHF level. With regard to the different effects of electron correlation on **1–4**, such an analysis would not be without bias.

deformations of $CH_3^+$ require significant amounts of energy (>20 kcal/mol), but the range of the $\Delta E(CH_3^+)$ values is narrow (<6 kcal/mol) compared to the methyl cation affinities of XY. Thus, the major differences in the reaction energies leading to 1–4 are caused by differences in the electronic relaxation associated with the combination of the profragments (eq 3). The energy values $\Delta E_{pro}$ have the quality of charge-transfer energies, and this charge transfer can be studied via the electron density difference function $\Delta\rho$.

The $\Delta\rho$ function for 1 shows electron transfer from the $N_2$ group into the $CH_3$ sp³-type region, which leads to electron depletion in the CH-bonding regions. The strong internal $N_2$ polarization is clearly visible, and in particular, the area of electron depletion at $N_\alpha$ shows that the "$N_\alpha$ σ lone pair" was moved into the CN-bonding region. Important characteristic differences occur regarding the electron density accumulation in the CX-bonding regions of 1–4. The shapes of the $\Delta\rho = 0$ contour may be used to typify these situations, where the arrows point to the atom toward which the density is polarized. The extreme of situation B would be cation solvation, and the extreme in the opposite direction would be a carbanion in an ion pair. The "shared"



**B**        **A**        **C**
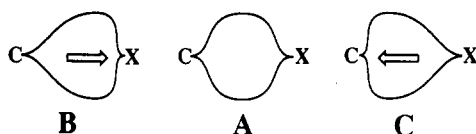
electron density in that region is polarized toward $X_\alpha$ for 1 and 3 (type B), but it is polarized toward C in 2 and 4 (type C). It is this polarization that results in the zero-flux surface characteristics that lead to the assignment of positive charge mainly to the $CH_3$ group in the CN compounds and to the XY group in the CP compounds in the topological partitioning scheme. Significant differences are found in the polarization patterns of the $X_\alpha$ atoms. The $CH_3$ group causes an increase of the $N_\alpha$ π-type density in the $N_\alpha-Y_\beta$ bonding region. In 2 and 4, this effect in the $P_\alpha$ π system also occurs but much weaker and, instead, there is a small response of this type in the σ system. Relatively small changes are found in the XY-bonding regions of 2–4. Small differences in these small changes caused by dependencies on the theoretical model are responsible for the large model dependency of the internal XY polarization, as indicated by the integrated properties (vide supra). We emphasize that the effects of the theoretical model on the electron density distributions in those regions are less than the derived integrated values suggest.

**Charge Distributions and Valence Bond Structures.** Considering the structural properties, the topological properties, and the analysis of the $\Delta\rho$ functions of 1–4, the charge distributions might best be represented as
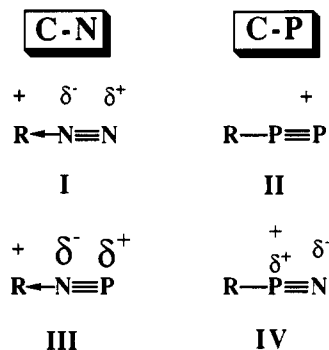


There is a clear distinction between the CN- and the CP-bonded ions. In the CN-bonded ions, the positive charge is largely located on the alkyl fragment and the XY group is polarized in a way that maximizes the charge dipole interaction between the frag-

ments. The degree of internal polarization depends on the electronegativity difference of X and Y. P substitution in the α position of I changes the charge distribution fundamentally: The charge resides on the XY group in CP-bonded ions. A moderate internal polarization of the type found for I and III persists for II while N in the β position leads to localization of the charge on $P_\alpha$. For the CP-bonded ions, the best Lewis structure *does* represent the charge distribution adequately, while the Lewis structures I and III for the CN-bonded ions *do not* appropriately reflect the charge distributions. In other words, the ions with CX bonds with the polarization type C are well represented by the Lewis structures while those with CX bonds with the polarization type B are not. *The crucial difference lies with the different degree by which the "X lone pair" is polarized toward (type B) or shared with (types A and C) carbon.*

## Conclusion

These results suggest that methyldiphosphonium ion (2) and methylphosphoazonium ion (3) should be stable ions that can be formed by combination of $P_2$ and PN with $CH_3^+$ in the gas phase. P methylation of PN should be greatly disadvantaged and, if it occurs at all, the methylazophosphonium ion 4 is predicted to easily isomerize to 3. Ions 2 and 3 remain thermodynamically stable with regard to C–X dissociation even if the oligomerizations of $P_2$ and PN are taken into account. Both 2 and 3 are predicted to be intrinsically more stable toward C–X dissociation than is the methyldiazonium ion 1. Qualitative features of the potential energy surfaces of protonated[18,20–23] $N_2$ and PN carry over to the methylated systems, but protonation and methylation of $P_2$ result in qualitatively different connectivities, and relative energies and cation affinities differ greatly in all cases. Similarly, deductions from the results for the *methyl* derivatives regarding *alkyl* derivatives in general might not be straightforward. We have shown earlier that methyl- and ethyldiazonium ions show a remarkable difference in their CN bond stabilities.[10] Considering the similar bonding patterns in 1 and 3, such pronounced effects also might be anticipated for 3. On the other hand, alkyldiphosphonium ions may be expected to resemble 2 since the CP bond is less polar. In any case, the effects of variation of the hydrocarbon fragment (alkanyl, alkenyl, alkinyl, and aryl) require further studies.

Alkyldiazonium ions can be detected not only in the gas phase but also in superacid media. The intrinsic stabilities of 2 and 3 toward C–X dissociation are an important prerequisite for their accessibility in superacidic media, and their preparation and detection poses an exciting challenge. The approach pioneered by Niecke et al.[5,6] for *aryl* derivatives of 3 might also be successful for the *alkyl* derivatives. Diphosphonium ions might be accessible by protonation of the (unknown) P analogues of diazo compounds, by Lewis acid catalyzed X elimination from diphosphenes RP=PX, or by direct alkylation of phosphorus. To examine these possibilities, the electronic structure analyses presented need to be extended to studies of the effects of specific solvation and to studies of possible reactions of the ions. Studies of these processes are in progress.